A Novel 3T1R Parallel Manipulator 2PaRSS and Its Kinematics

Huiping Shen[1]*，Guowei Shao[2]，Jiaming Deng[3], Ting-li Yang[4]

[1] School of Mechanical Engineering, Changzhou University，213164，Jiangsu,P.R.China, e-mail: shp65@126.com*
[2]School of Mechanical Engineering, Changzhou University，213164，Jiangsu,P.R.China, e-mail: 898618909@qq.com
[3]School of Mechanical Engineering, Changzhou University，213164，Jiangsu,P.R.China, e-mail: czdydjm@126.com
[4]Research Center for Advanced Mechanism Theory, Changzhou University，213164，Jiangsu,P.R.China, e-mail: yangtl@126.com

Abstract. By using the topological structure synthesis theory and method based on POC (Position and Orientation Characteristic) equations，a novel 4-DOF 3T1R parallel manipulator (PM) with low coupling degree, **2PaRSS**, is presented．First，the modeling and numerical solutions for forward and inverse position of the PM is established. Then, the workspace and rotation capacity of the PM are analyzed based on inverse solutions. This work shows 2PaRSS has simple structure, larger workspace and rotation capacity comapered to H4, I4 etc.

Key words*:* Parallel manipulator, POC, Coupling degree, Kinematics, SOC

1 Introduction

On type synthesis of three-translation and one-rotation (3T1R) PMs, F.Pierrot and O.Company *et al.* proposed a class of famous 4-DOF parallel robots that have been widely industrial used such as H4[1], I4L[2], I4R[3], Par4[4] and Heli4[5], all of those are composed of four identical complex chains containing a parallelogram between the static and moving platform. Meanwhile, the coupling degrees of all these PMs mentioned are larger, which are k =2[6].

The coupling degree is used to describe the complexity of the topological structure of a mechanism[7]. It is represented by k ($k\geq 0$) that reflects the independence of the kinematic variables among loops of a PM, and also reflects the complexity of kinematics and dynamics solutions for the mechanism. It has been proved that the larger the value k, the higher of the complexity will be[6,7,8]. Therefore, the

forward position solutions of all these existing 3T1R PMs are very difficult, which influences their real-time control and path planning.

By using topological structure synthesis theory and method for PMs based on POC equations[6,8], the authors proposed a class of novel 4-DOF 3T1R PMs[6]. Among them, one is a novel **2PaRSS** PM presented in this paper. The PM features simple structutre, large workspace and rotational ability. But its coupling degree is low, i.e., k =1. The PM is composed of only two parallelogram complex chains containing 4S and two nonconstraint RSS chains(S-spherical joint, R-rotation joint). Therefroe, the PM is not only simpler in the structure but also easier both in the solutions for kinematics and dynamics and in manufacturing as well as assembly than that of H4 etc. The reason is that these existing PMs contain four parallelogram complex chains containing 4S and their coupling degrees are larger (k =2) [6].

2 Structural analysis

As shown in Fig.1, the **2PaRSS** PM [6,9] consists of a moving platform 1, a static platform 0, two nonconstraint RSS chains and a hybrid chain whose end link 2 produces three-translation output.

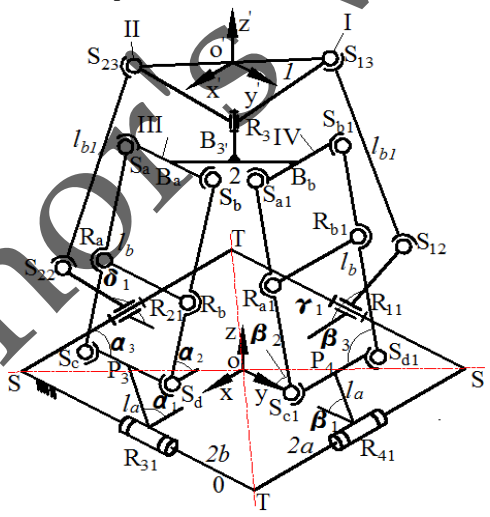

Fig.1 A novel **2PaRSS** PM and kinematic modeling

The hybrid chain has two parallelogram sub-chains III and IV which have four spherical joints (S_a,S_b,S_c,S_d) connected by the link 2. A rod with two rotating joints R_a and R_b shall be in the parallelogram configuration to make the four joints S_a, S_b, S_c, S_d in the same plane. The length of the rod R_aR_b is equal to S_aS_b or S_c,S_d. The axis of the rotation pair R_3 must be perpendicular to the moving platform 1.

Joint R_{11}, R_{21}, R_{31} and R_{41} are four actuated joints, and they are located in the midpoint of each side in the static platform 0. Two parallelogram sub-chains should satisfy $R_{31} \perp R_{41}$, while two nonconstraint RSS chains may take any arrangement relation, say $R_{11} \perp R_{21}$. "⊥" stands for perpendicular. Thus, the moving platform 1 can realize three translations and one rotation around the R_3 axis[6].

The topological analysis for the **2PaRSS** PM can be found in [6], which shows that the PM contains only one Assur Kinematic Chain (AKC) and its coupling degree is only 1. Therefore all of the numerical solutions for the forward position can be found by using one dimensional search method.

3 Position analysis

3.1 The coordinate system and annotation

Given the input angles ($\alpha_1, \beta_1, \gamma_1, \delta_1$) of the actuated joints, the forward position solution is to solve the position (x, y, z) and the attitude angle (γ) of the moving platform 1, as in Fig.1.

The static coordinate system O-XYZ is in the geometric center of the static platform 0, X axis is collinear with the connection line between R_{11} and R_{31}, Y axis is collinear with the connection line between R_{21} and R_{41}, and the direction of Z axes are determined by the law of the right hand. The origin of the coordinate o'-X'Y'Z' is located in the midpoint of the hypotenuse ($S_{13}S_{23}$) of the platform 1, X' axis is parallel to the connection line between S_{13} and R_3, and Y' axis is parallel to the connection line between S_{23} and R_3. Since the static platform 0 is rectangular, its length and width are *2a* and *2b* respectively. Moving platform 1 is isosceles right triangle and the length of the right side is $2m_2$.

The orientation angle γ is the rotation angle of the moving platform 1 around the rotation pair R_3, which is expressed by the angle between the OX axis and the connection line from R_3 to o'. The counter-clockwise direction of the angles is positive. The point $B_{3'}$ is the midpoint of the rod B_aB_b. Let $R_3B_3 = q_1$, $B_aB_b = l$. The angle between the B_aB_b and the rod of S_aS_b or $S_{a1}S_{b1}$ is φ, respectively. Let $R_{11}S_{12}=R_{21}S_{22}=l_{a1}$, $S_{12}S_{13}=S_{22}S_{23}=l_{b1}$, $R_{31}P_3=R_{41}P_4=l_a$, $P_3B_a=P_4B_b=l_b$.

The angles between the parallelogram plane and the static platform plane are α_2 and β_2 respectively, while the interior angles of two parallelograms are respectively α_3 and β_3, as shown in Fig.1.

The position of the rod $S_{13}S_{12}$ and $S_{23}S_{22}$ in the space are expressed by three angles between them with the X, Y, Z axes in the static platform 0 respectively, which are $\gamma_2,\gamma_3,\gamma_4$ and $\gamma_5,\gamma_6,\gamma_7$, as shown in Fig.2.

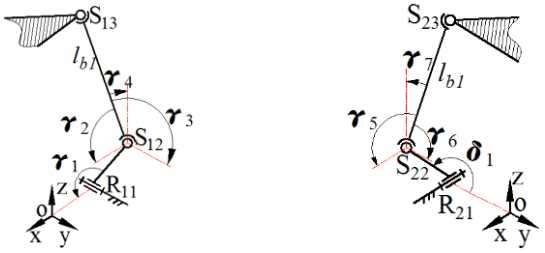

（a）chain I （b）chain II

Fig.2 Calculation model of chain I and II

3.2 *Forward position modeling*

The principle of modeling of forward position analysis based on SOC mthod can be found in[8].

3.2.1 The modeling of the SOC1

1) The first SOC, i.e.SOC_1, of the PM is composed of two sub-chains III and IV, joint R_3 and S_{13}-S_{12}-R_{11} chain, as in Fig.1. By SOC_1, the coordinates of point O ', S_{13}, S_{23} can be obtained by D-H matrix as follows

$$\begin{bmatrix} x_{o'} \\ y_{o'} \\ z_{o'} \end{bmatrix} = \begin{bmatrix} a - l_a\cos\alpha_1 - l_b\sin\alpha_3\cos\alpha_2 - l/2\cos\varphi - \sqrt{2}m_2\cos(\pi/4+\gamma) \\ l_b\cos\alpha_3 - l/2\sin\varphi - \sqrt{2}m_2\sin(\pi/4+\gamma) \\ l_a\sin\alpha_1 + l_b\sin\alpha_3\sin\alpha_2 + q_1 \end{bmatrix} \quad (1)$$

$$\begin{bmatrix} x_{o'} \\ y_{o'} \\ z_{o'} \end{bmatrix} = \begin{bmatrix} l_a\cos\beta_3 + l/2\cos 45^0 - \sqrt{2}m_2\cos(\pi/4+\gamma) \\ -l_a\cos\beta_1 - l_b\sin\beta_3\cos\beta_2 - l/2\sin 45^0 - \sqrt{2}m_2\sin(\pi/4+\gamma) \\ l_a\sin\beta_1 + l_b\sin\beta_3\sin\beta_2 + q_1) \end{bmatrix} \quad (2)$$

$$\begin{bmatrix} x_{S_{13}} \\ y_{S_{13}} \\ z_{S_{13}} \end{bmatrix} = \begin{bmatrix} a - l_a\cos\alpha_1 - l_b\sin\alpha_3\cos\alpha_2 - l/2\cos\varphi - 2m_2\cos\gamma \\ l_b\cos\alpha_3 - l/2\sin\varphi - 2m_2\sin\gamma \\ l_a\sin\alpha_1 + l_b\sin\alpha_3\sin\alpha_2 + q_1 \end{bmatrix} \quad (3)$$

$$\begin{bmatrix} x_{S_{23}} \\ y_{S_{23}} \\ z_{S_{23}} \end{bmatrix} = \begin{bmatrix} a - l_a\cos\alpha_1 - l_b\sin\alpha_3\cos\alpha_2 - l/2\cos\varphi - 2m_2\cos\gamma \\ l_b\cos\alpha_3 - l/2\sin\varphi - 2m_2\sin\gamma \\ l_a\sin\alpha_1 + l_b\sin\alpha_3\sin\alpha_2 + q_1 \end{bmatrix} \quad (4)$$

By using Eq. (1) and (2), we have the equation as

$$(k+t_1)k_1^2 + 2t_3k_1 + k - t_1 = 0$$

Then we get

$$k_1 = \frac{-t_3 \pm \sqrt{t_3^2 - k^2 + t_1^2}}{k + t_1}$$

where $k_1 = \tan\alpha_2/2$ （5）

$$t_1 = a - l_a\cos\alpha_1 - l\cos\varphi;\ t_2 = -l_a\cos\beta_1;\ \ t_3 = l_a\sin\alpha_1 - l_a\sin\beta_1$$

$$k = \frac{t_1^2 + t_2^2 + t_3^2 - 2t_2 l_b\cos\alpha_3}{2l_b\sin\alpha_3}$$

We assign the angle α_3 as the virtual variable, i.e. α_3^*. Then, by Eq. (5), α_2 is a function of the virtual variable α_3^*.

2) By the chain I, as in Fig.2, the coordinates of S_{12} can be easily obtained. Further, by Eq.(3) and the link-length constraint $S_{12}S_{13} = l_{b1}$, we can obtain

$$A_1\sin\gamma + B_1\cos\gamma + C_1 = 0$$

Where

$A_1 = -4m_2(l_b\cos\alpha_3 - l/2\sin\varphi)$;

$B_1 = -4m_2(a - l_a\cos\alpha_1 - l_b\sin\alpha_3\cos\alpha_2 - l/2\cos\varphi + l_{a1}\cos\gamma_1)$;

$C_1 = (a - l_a\cos\alpha_1 - l_b\sin\alpha_3\cos\alpha_2 - l/2\cos\varphi + l_{a1}\cos\gamma_1)^2 +$

$(2m_2)^2 + (l_b\cos\alpha_3 - l/2\cos\varphi)^2 + (l_a\sin\alpha_1 + l_b\sin\alpha_3\sin\alpha_2 + q_1 - l_{a1}\sin\gamma_1)^2 - l_{b1}^2$;

And let

$$k_2 = \tan(\gamma/2) \qquad (6)$$

We have

$$k_2 = \frac{-A_1 \pm \sqrt{A_1^2 + B_1^2 - C_1^2}}{C_1 - B_1} \qquad (7)$$

It is known from Eq.(6) and (7) that angle γ^* is also a function of virtual variable α_3^*.

3.2.1 The modeling of SOC_2

The second SOC, i.e.,SOC_2, is S_{23}-S_{22}-R_{21}, as in Fig.2, by which the coordinates of S_{22} are easily obtained. Further, according to Eq.(4) and the link-length constraint $S_{22}S_{23} = l_{b1}$, we have

$$f(\alpha_3^*) = (a - l_a\cos\alpha_1 - l_b\sin\alpha_3^*\cos\alpha_2^* - l/2\cos\varphi + 2m_2\sin\gamma^*)^2$$
$$+ (l_b\cos\alpha_3^* - l/2\sin\varphi - 2m_2\cos\gamma^* - l_{a1}\cos\delta_1)^2 + (l_a\sin\alpha_1 + l_b\sin\alpha_3^*\sin\alpha_2^* + q_1 - l_{a1}\sin\delta_1)^2 - l_{b1}^2 \qquad (8)$$

By continuously changing α_3^* from 0 to 360 until $f(\alpha_3^*) = 0$, the value of α_3 is the real value. Then, the coordinates of point O', $o'(x, y, z)$, can be obtained when the real α_3 is substituted into Eqs.（1）and（5）. Further, by taking into Eq. (6), the real angle γ of the moving platform 1 can be obtained.

When the position (x, y, z) and angle γ of the moving platform 1 are known, the input angle $\alpha_1, \beta_1, \gamma_1, \delta_1$ of the driving arm is easily solved, which is the inverse

position solutions for the PM. Both the forward and inverse position solutions of **2PaRSS** PM have been testified to be correct by using an numerical example, which is omitted for the limited space.

4 Workspace and rotation capacity analysis

The method of limit boundary searching based on inverse position solutions [10] is used to analyze the workspace of the **2PaRSS** PM. Namely, the height in the Z direction of the workspace is pre-determined, the boundary of workspace will be found by changing the search radius ρ and angle θ .This paper chooses the parameters such as $550 \le z \le 1200$ and $\Delta z = 10$, $-\pi \le \theta \le \pi$, $0 \le \rho \le 1000$. The range of the input angle $\alpha_1, \beta_1, \gamma_1, \delta_1$ are $[0, \pi]$.

4.1 Workspace analysis

Using the MATLAB, the three-dimension graph of the workspace of the **2PaRSS** is shown in Fig.3, and each X-Y cross-section is shown in Fig.4. We find:

(a) When 400mm≤z≤550mm, the internal space has an empty hole. The empty hole will disappear while increasing height Z.

(b) When $z \in [550,1000]$, the X-Y cross-section of the workspace is symmetric about the T-T line.

(c) The workspace is a regular one, while increasing Z, the cross-section area will decrease.

(d) Without considering the interference of the links, the workspace is bigger than that of I4R (H4) etc in the same parameters and the search scope. The specific data are as follows:

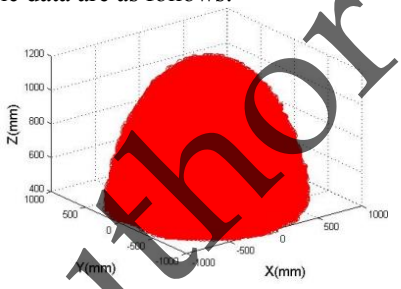

Fig. 3 Workspace of 2PaRSS

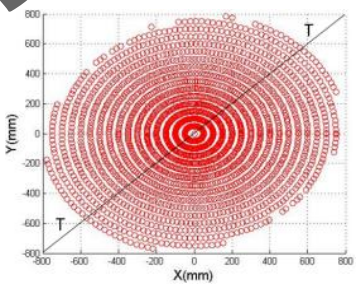

Fig.4 X-Y section of workspace when Z=850mm

① Using the parameters of [11] and giving the search scope such as $0 \le \rho \le 1000$ and $500 \le z \le 1150$, the workspace volume of I4R is 6.1668*10^8（mm^3）, and that of **2PaRSS** is 7.0070*10^8（mm^3）. Therefore, the workspace of **2PaRSS** is increased by 13.6% compared to I4R robot.

②Using the parameters of [12], the workspace volume of CrossIV-3 is 4.4274*10^8（mm^3）and that of the **2PaRSS** is 4.6464*10^8（mm^3）. Therefore, the workspace of **2PaRSS** is increased by 4.95% compared to CrossIV-3 robot.

4.2 Rotation capacity analysis

The rotation capacity of the moving platform is defined as the rotation range of the end effector in the workspace[13]. Its size is also an important indicator to measure the rotating performance of the **2PaRSS** PM.

Considering the scope of $z \in [550,1000]$, at any X-Y cross-section, we can get the rotation ability of the moving platform. For clarity, we use z=1000mm as an example. Then the X-Y cross-section of the **2PaRSS** is got as shown in Fig.5. And the rotation capacity of H4 is shown in Fig.6, from which we observe as follows:

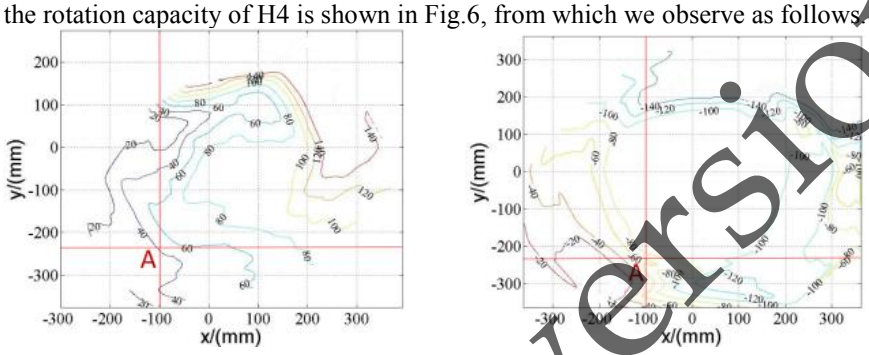

(a) Distribution of $\gamma_{\max}$ (b) Distribution of $\gamma_{\min}$

Fig. 5 Rotational capacity of 2PaRSS when Z=1000mm

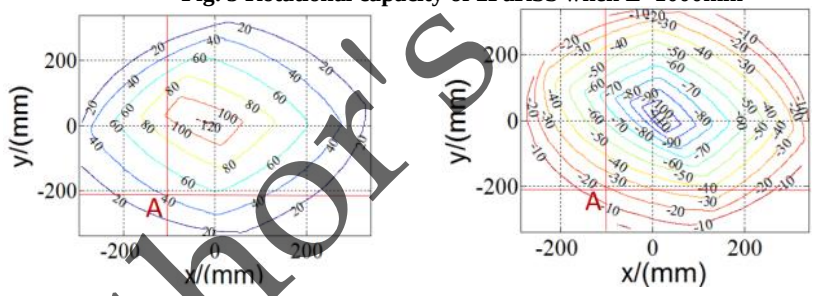

(a) Distribution of $\gamma_{\max}$ (b) Distribution of $\gamma_{\min}$

Fig. 6 Rotational capacity of H4 when Z=1000mm

The rotation range of the **2PaRSS** in the X-Y plane is $-140^0 \le \gamma \le +140^0$ when z=1000, while the rotation range of H4 is $-120^0 \le \gamma \le +110^0$. Comparing with H4, the distribution of $\gamma_{\max}$ is increased by 30º, and the distribution of $\gamma_{\min}$ is increased by 20º. Therefore, the total value of **2PaRSS** will increase by 21.74% relative to H4. Specific comparisons are given as follows:

When using the point $A(-100,-237,1000)$ as an example, the rotation output of the H4 is $\gamma_{\max} = 40^0$ and $\gamma_{\min} = -20^0$, while **2PaRSS** is $\gamma_{\max} = 40^0$ and $\gamma_{\min} = -60^0$. Therefore, it is easy to find that rotation capacity of the **2PaRSS** is larger than that of H4.

5 Conclusions

A novel 4-DOF 3T1R **2PaRSS** manipulator with simple structure and low coupling degree is presented.

The modeling of the forward position solutions based on the SOC method is established. A position constraint equation (Eq.(8)) with only one variable is derived, from which all numerical solutions of forward position are obtained by using one-dimension search method.

Based on inverse position solutions, the performance of the workspace is also analyzed. It is proved that the workspace of the **2PaRSS** is increased by 13.6% and 4.95% respectively compared with that of H4(I4) etc. The rotation capacity of the **2PaRSS** is increased by 21.74% compared with that of H4. This work shows the **2PaRSS** PM has potential applications.

Acknowledgments This research is sponsored by Jiangsu Key Development Project (No.BE2015043) and Jiangsu Scientific and Technology Transformation Fund Project (No. BA2015098) and NSFC (No. 51475050, 51375062) .

References

[1] Pierrot F. H4: a new family of 4-DOF parallel robots. 1999. In: Proceedings of 1999 IEEE/ASM E International Conference on Advanced Intelligent Mechatronics, pp.508-513 (1999).

[2] Krut S, Benoit M, Ota H, et al. I4: A new parallel mechanism for Scara motions. In: Proceedings of IEEE International Conference on Robotics and Automation, pp.2: 1875-1880 (2003).

[3] Krut S, Nabat V,Pierrot F. A high-speed parallel robot for Scara motions. In: Proceedings of 2004 IEEE International Conference on Robotics and Automation, pp. 4: 4109-4115(2004)

[4] Nabat V,de la 0 Rodriguezm, Krut S, et al. Par4: very high speed parallel robot for pick-and-place). In: Proceedings of 2005 IEEE/RSJ International Conference on Intelligent Robots and Systems,pp.553-558 (2005).

[5] Krut S, Nabat V,Pierrot F. Heli4: A Parallel Robot for Scara Motions with a Very Compact Traveling Plate and a Symmetrical Design. In: Proceedings of International Conference on Intelligent Robots and Systems, pp.1656-1661 (2006).

[6] Yang Tingli，Liu Anxin，Shen Huiping，Hang Lubin， Topological structure synthesis of 3T1R parallel mechanism based on POC equations**.** In: Proceedings of 9th International Conference on Intelligent Robotics and Applications,Lecture Notes in Computer Science, v9834, pp.147-161, ICIRA 2016.P.147-161 DOI: 10.1007/978-3-319-43506-0_13 (2016)

[7] Yang T. L. Structural Analysis and Number Synthesis of Spatial Mechanisms，In: Proceedings of the 6th World Cong. on Mechanisms and Machines Theory. New Delhi,pp.1.280-283(1983).

[8] YANG Tingli．Topology structure design of robot mechanisms．China Machine Press(2004).

[9] Shen Huiping，YangTingli，Shao Guowei，et al．A parallel robot hand with three translations and one rotation．Patent application number：201510640394．X(2015).

[10] Xu Zonggang.Studies and application of workspace and trajectory Planning for3-PCR parallel mechanism. SHANDONG UNIVERSITY OF TECHNOLOGY(2009).

[11] Liu Pingsong. Study on global performance and optimization of I4R parallel robot. Nanjing: Nanjing University of Science and Technology(2013)

[12] LI Yuhang MEI Jiangping LIU Songtao et al. Dynamic dimensional synthesis of a 4-DOF high-speed parallel manipulator.CHINESE JOURNAL OF MECHANICAL ENGINEERIN, 19, pp.32-40(2014).

[13] Xie F, Liu X J. Design and Development of a High-Speed and High-Rotation Robot With Four Identical Arms and a Single Platform. Journal of Mechanisms & Robotics, pp. 7(4).(2015)